Generation and Structure of Solitary Rossby Vortices in Rotating Fluids

Nikolai Kukharkin* and Steven A. Orszag
Fluid Dynamics Research Center, Princeton University, Princeton, New Jersey 08544
(February 5, 2008)

The formation of zonal flows and vortices in the generalized Charney-Hasegawa-Mima equation is studied. We focus on the regime when the size of structures is comparable to or larger than the deformation (Rossby) radius. Numerical simulations show the formation of anticyclonic vortices in unstable shear flows and ring-like vortices with quiescent cores and vorticity concentrated in a ring. Physical mechanisms that lead to these phenomena and their relevance to turbulence in planetary atmospheres are discussed.

PACS numbers: 47.27.-i, 92.60 Ek

Fluid motion subject to strong rotation, stratification, or action of a magnetic field can often be considered as quasi-two-dimensional. One of the major features of 2D flows is their tendency to self-organization which reveals itself by spontaneous generation of coherent structures (e.g. vortices, jets) that dominate the large-scale motion. The dynamics of these structures becomes more complicated when the inverse energy cascade interferes with the characteristic spatial scale determined by the external field. The presence of the Coriolis force due to rotation (β-effect) leads to a limitation on vortex sizes in the meridional direction by the Rhines length [1], while in the strong turbulence regime when waves are neglected, the influence of the finite deformation (Rossby) radius results in the emergence of "shielded" vortices, which can form a quasicrystalline structure [2].

In this Communication we extend previous studies to include both wave and finite deformation radius effects, so that the model becomes more relevant to geophysics and plasma physics applications and reveals new physical effects. It is known from observations that, in planetary atmospheres, there exist global-scale circulations in the form of longitudinal zonal flows with embedded long-lived vortices. Indeed, this effect is significant in the atmospheres of giant planets and in the Earth's oceans. The mechanism of the formation of zonal flows on the surface of giant planets is a separate question which is not well understood. Two distinct approaches to this problem are based respectively on 3D thermal convection [3] and on the inverse energy cascade in 2D turbulence. Very recent data obtained by the Galileo probe during the unique first-ever *in situ* measurements in the atmosphere of Jupiter [4] seem to be more in favor of the 3D convection concept: the observations showed stronger than previously assumed winds (up to 200 m/s) and turbulence in the upper layer of the Jovian atmosphere. This indicates that the origin of Jupiter's winds and circulation patterns is probably heat escaping from Jupiter's deep interior. However, the eddies we are interested in here are believed to be quasi-2D structures originated from the instability of zonal flows and confined to a shallow atmospheric layer.

There have been several studies devoted to the combined impact of finite deformation radius and the β-effect [5,6]. However, it is difficult to detect any particular new physical effects, since the scales overlap thus making the whole picture vague. If the rotation is strong enough, zonal flows destroy coherent vortices. In the opposite case, when the deformation radius is smaller than the Rhines length, the formation of "shielded" weakly interacting vortices significantly reduces the inverse cascade, so that zonal flows do not form. We will show how this difficulty can be partly overcome if the simplistic model is modified to take into account additional effects that take place when scales of the order or larger than the deformation radius are considered.

We consider the generalized geostrophic (or Charney-Hasegawa-Mima) equation for Rossby-wave turbulence in the β-plane approximation:

$$\partial_t(\nabla^2 h - \lambda^2 h) + [h, \nabla^2 h] + \beta\partial_x h(1+h) = D + F, \quad (1)$$

where λ is the ratio of a spatial scale used for normalization to the Rossby radius $L_R = (gH_0)^{1/2}/f_0$, g is the gravitational acceleration, $h = (H - H_0)/H_0$ is the perturbation of the atmosphere of average depth H_0, $f = f_0 + \beta y$ is the Coriolis parameter, $[a, b] = a_x b_y - a_y b_x$, D and F is the dissipation and forcing respectively, and the following dimensionless variables are used: $x, y \to \lambda L_R x,\ \lambda L_R y,\quad t \to \lambda^2 t/f_0,\quad \beta \to f_0\beta/\lambda^3 L_R$. Eq.(1) is isomorphic to the equation for drift waves in a magnetized plasma where the inhomogeneity of the Coriolis parameter is replaced by the gradient of the electron density (see, e.g., [7] for details). Consequently all results can be transferred to the plasma case. The equation containing the quadratic β-term was derived for the first time in [8] and has been studied since then for various applications [9]. The presence of the scalar nonlinearity $\beta h\partial_x h$ is known to introduce cyclone/anticyclone asymmetry in Eq.(1) (in a cyclone the direction of rotation coincides with that of the system). This term appears due to the perturbation of the fluid depth under the influence of the Rossby wave, so that the full depth $H = H_0 + h$ should be retained rather than the mean depth H_0.

Studies of shear flows formed due to the strong rotation in β-plane 2D models indicate that these flows are stable as described by the Rayleigh-Kuo instability criterion [10,11]. This result obviously contradicts the observed

coexistence of coherent long-lived vortices and zonal jets in the Jovian atmosphere. Following [9] we show that this contradiction can be resolved when the finite deformation radius is taken into account. The Rayleigh-Kuo criterion for shear flow instability in the approximation of a constant depth of the atmosphere ($H_0 = const$) is given by $\partial^2 U/\partial y^2 - \beta_0 = 0$, where U is the average horizontal flow velocity, y is the meridional coordinate, and $\beta_0 = \partial f/\partial y$. However, if there is a free surface, the average depth of the atmosphere H_0 can change in the meridional direction: $\partial H_0/\partial y \neq 0$. This gradient is balanced by the Coriolis force $g\partial H_0/\partial y = -fU$, and β is given by

$$\beta = -\frac{1}{L_R^2}\frac{\partial}{\partial y}(fL_R^2) = \frac{\partial f}{\partial y} - \frac{f}{H_0}\frac{\partial H_0}{\partial y} = \beta_0 + \frac{U}{L_R^2} \quad (2)$$

Consequently, the modified instability criterion is [9]

$$\frac{\partial^2 U}{\partial y^2} - \beta_0 - \frac{U}{L_R^2} = 0 \quad (3)$$

or in our dimensionless units

$$\frac{\partial^2 U}{\partial y^2} - \beta_0 - \lambda^2 U = 0 \quad (4)$$

It is now clear that zonal flows which otherwise would be stable can become unstable when the finite deformation radius is taken into account. At the same time, the scalar nonlinearity in Eq.(1), as in the case of the Korteweg-de Vries equation, can lead to the gradual steepening of the initial perturbation in the longitudinal direction which is compensated by negative dispersion only for anticyclones. One can thus expect that vortices emerging due to the instability of zonal flows will be mostly anticyclones.

We used the following setup for the numerical experiment to check this prediction. In 2D turbulence it has been convincingly demonstrated that the case in which long-term dynamics does not depend on initial conditions is best achieved with small-scale random forcing. In this case zonal flows are known to be a robust feature of the flow evolution on the β-plane. We solve Eq.(1) numerically using a pseudospectral method in a square domain $2\pi \times 2\pi$ with doubly periodic boundary conditions and resolution 512×512. To confine the dissipation to the smallest scales we use hyperviscosity $D = (-1)^{p+1}\nu_p \nabla^{2p}(\nabla^2 h)$, $p = 8$. We start with zero initial conditions, random forcing at $100 < k_f < 105$, and $\beta = 100$, $\lambda = 0$. One can expect the formation of zonal flows to begin when the inverse energy cascade reaches the Rhines scale $L_\beta \simeq k_\beta^{-1}$, $k_\beta = (\beta^2/\epsilon)^{1/5}$, where ϵ is the energy injection rate, and in the considered case $k_\beta \simeq 60$. The flow is dominated by well-developed zonal flows by $t = 15\tau_0$, where $\tau_0 \simeq \pi/v_{rms}$ is the large eddy turnover time. At this moment the force is turned off to let the viscosity smooth out the irregularities in the smallest scales. At time $t = 17\tau_0$ one can observe quite regular shear flows. The horizontal velocity has a profile resembling the one on Jupiter with smooth westward and peaked eastward flows (Fig. 1a). These flows are stable, since $U_{yy} - \beta_0 < 0$ for all y (Fig. 1b). After that we "turn on" the deformation radius (or equivalently remove the "rigid lid" and allow the fluid to have a free surface) by taking $\lambda = 10$. The choice of λ is made such that the parameters would be close to the ones for Jupiter's Great Red Spot (JGRS). For Jupiter $R/L_R \simeq 7 \cdot 10^4 km/6 \cdot 10^3 km \sim 10$, $f_{GRS} \simeq 1.4 \cdot 10^{-4} s^{-1}$, and since $\beta \sim f/R$, this gives $\beta \simeq 100$ in our dimensionless units. The value $U_{yy} - \beta_0 - \lambda^2 U$ now changes sign for some y, and the westward anticyclonic ($U < 0$) zonal flow become unstable. This almost immediately ($\Delta t \sim \tau_0$) leads to the formation of vortices. They presumably appear as cyclone-anticyclone pairs with cyclones decaying faster, so that only anticyclones survive (Fig.2). To illustrate the asymmetry of the solution, in Fig.3 we plot the vorticity skewness $S_\omega(t) = \langle \omega^3 \rangle / \langle \omega^2 \rangle^{3/2}$, where $\omega = \nabla^2 h$, $\langle \ \ \rangle$ denotes an area average ($\omega < 0$ corresponding to anticyclones).

Another important feature to verify is the form of the vortices. As was discussed in [8,12] the scalar nonlinearity in Eq.(1) allows soliton-like solutions. These solutions combine characteristic features of both waves and real vortices, in the sense that they have trapped fluid, so they are called "solitary vortices". An analytically obtained solution [8] under the assumption $h \ll H_0$ predicts the structure of such a soliton to be given by

$$h/h_0 = cosh^{-3/4}(\frac{3r}{4a}), \quad a \simeq L_R h_0^{-1/2} \quad (5)$$

Consequently, the vorticity profile $\omega = \nabla^2 h = \frac{1}{r}\frac{\partial}{\partial r}(r\frac{\partial h}{\partial r})$ is smooth, gradually decreasing (increasing) from the center of a vortex. Observations show, however, that, for example, the JGRS and intrathermoclinic vortices (lenses) in the Earth's ocean do not rotate as solid bodies, and their vorticity has a circumferential profile with a rotating perimeter and relatively quiet core. Also in experiments in rotating tanks [13] with $h \simeq O(1)$, vortices appear to be more localized than predicted by the theoretical solution (5). Sutyrin noted [14] that much better agreement with experiments can be obtained if one uses the assumption that there is a uniform profile of the potential vorticity $\xi = \nabla^2 h - \lambda^2 h = const$ inside the vortex, although the vorticity profile was never analyzed. Ironically, Marcus [15] used the same assumption to criticize the soliton-like model, arguing that it is unable to produce ring vortices.

We show here that the model Eq.(1) does produce ring vortices and we present the evidence that it is the scalar nonlinearity that plays a decisive role. It is important to emphasize that these vortices spontaneously arise from random initial conditions; they are not in any sense "trial" vortices introduced into the flow.

In our numerical experiment without forcing we start with the following initial perturbation

$$h_{\mathbf{k}} = \begin{cases} Cexp(i\phi_{\mathbf{k}}) & \text{if } 4 < k < 5 \\ 0 & \text{otherwise,} \end{cases}$$

with random phases $\phi_{\mathbf{k}} \in [0, 2\pi)$. C is chosen such that total initial energy, $E = \frac{1}{2}\sum_k (k^2 + \lambda^2)|h_{\mathbf{k}}|^2$, is equal to 0.5, and $\lambda = L_R^{-1} = 10$, $\beta = 20$. The characteristic size of the initial eddies is $L \simeq (6 \div 7)L_R$. During the evolution of the system for over $50\tau_0$ we observe the formation of elongated vorticity sheets, which deform into loops. These loops could close into ring vortices, all of them being anticyclones (Fig.4). If the scalar nonlinearity is dropped from the equation, closed loops and ring vortices (in this case they could equally be cyclones and anticylones) do not form (Fig.5a). In the case $\beta = 0$ the cubic nonlinearity $J(h, h\nabla^2 h + \frac{1}{2}(\nabla h)^2)$ should be retained in Eq.(1) [5]. The cyclone/anticyclone asymmetry is then preserved, but no signs of ring vortices are found (Fig.5b).

We do not have a theoretical explanation of the formation of ring vortices, but necessary physical conditions can be identified. First of all, because of the finite deformation radius L_R vortices are shielded, i.e. their interaction decreases exponentially. This means that a ring vortex should be of the size of several L_R in order to be stable. Simultaneously, the Rhines length L_β and the Rossby radius L_R should be comparable; in the opposite case either zonal flows or "frozen", not mobile, vortices dominate the flow. Mutual action of negative dispersion and KdV-like scalar nonlinearity can lead to the formation of loops. Connection of the opposite sides of a loop leads to the formation of a ring vortex. Thus, both finite deformation radius and the scalar nonlinearity are crucial for the emergence and stability of ring vortices.

In conclusion, we have studied the question determining the combined influence of the β-effect (both Rossby waves and KdV nonlinearity) and deformation radius on coherent structures. It is shown that for a certain set of parameters (close to those of giant planets) large-scale zonal flows created by small-scale forcing tend to preferentially form anticyclonic vortices. Their emergence can be explained by the modified Rayleigh-Kuo instability criterion, which takes into account the deformation of free surface. We have provided numerical evidence that for scales larger than the Rossby radius, the scalar nonlinearity is responsible for the formation of ring anticyclonic vortices, a feature known from observations. We have demonstrated how gradual complication of the simple model allows one to clearly reveal new physical effects. The complete and accurate study of these effects will need simulations of more complicated equations on the sphere (in the spirit of [16,17]).

This work was partially supported by ARPA/ONR Grant N00014-92-J-1796.

* Electronic address: nnk@cfd.princeton.edu

[1] P.B. Rhines, J. Fluid Mech. **69**, 417 (1975).
[2] N. Kukharkin, S.A. Orszag, and V. Yakhot, Phys. Rev. Lett. **75**, 2486 (1995).
[3] F.H. Busse, Chaos **4**, 123 (1994).
[4] Science **272** (1996).
[5] B. Cushman-Roisin and B. Tang, J. Phys. Ocean. **20**, 97 (1990).
[6] L.M. Polvani *et al.*, Chaos **4**, 177 (1994).
[7] W. Horton and A. Hasegawa, Chaos **4**, 227 (1994).
[8] V.I. Petviashvili, Sov. Phys. JETP Lett. **32**, 619 (1980).
[9] M.V. Nezlin and E. N. Snezhkin, *Rossby Vortices, Spiral Structures, Solitons* (Springer-Verlag, Heidelberg, 1993) and references therein.
[10] G. K. Vallis and M.E. Maltrud, J. Phys. Ocean. **23**, 1346 (1993).
[11] A. Chekhlov *et al.*, Physica D, to appear (1996).
[12] J.G. Charney and G.R. Flierl, in *Evolution of Physical Ocenography*, ed. by B.A. Warren and C. Wunsch (MIT Press, Cambridge, 1981).
[13] S.V. Antipov *et al.*, Sov. Phys. JETP **55**, 85 (1982).
[14] G.G. Sutyrin, Dokl. Akad. Nauk SSSR **280**, 38 (1985).
[15] P.H. Marcus, Ann. Rev. Astron. Astrophys. **31**, 523 (1993); P.H. Marcus and C. Lee, Chaos **4**, 269 (1994).
[16] A. Gandhi, (unpublished, 1994).
[17] J.Y-K. Cho and L.M. Polvani, Phys. of Fluids **8**, 1531 (1996).

FIGURE CAPTIONS

Figure 1. Averaged zonal velocity U (a) and $U_{yy} - \beta$ (b) as functions of latitude y.

Figure 2. Finite deformation radius makes zonal flows unstable with respect to generation of anticyclones. The vorticity field before (a) and after (b) introducing a finite deformation radius L_R (whose scale is shown in the right picture). Darker colors correspond to the anticyclons.

Figure 3. Vorticity skewness $S_\omega(t)$, $\lambda = 0$ before $t = 15\tau_0$ and $\lambda = 10$ afterwards.

Figure 4. Instantaneous vorticity field at $t = 40\tau_0$ showing the ring anticyclonic vortices, $S_\omega = -2.8$ (a); cross section of a typical vortex (b).

Figure 5. Vorticity fields at the same time as in Fig.4 when (a) the scalar nonlinearity is dropped, $S_\omega = 0$; (b) $\beta = 0$, but the term $J(h, h\nabla^2 h + \frac{1}{2}(\nabla h)^2)$ is added, $S_\omega = -0.3$.

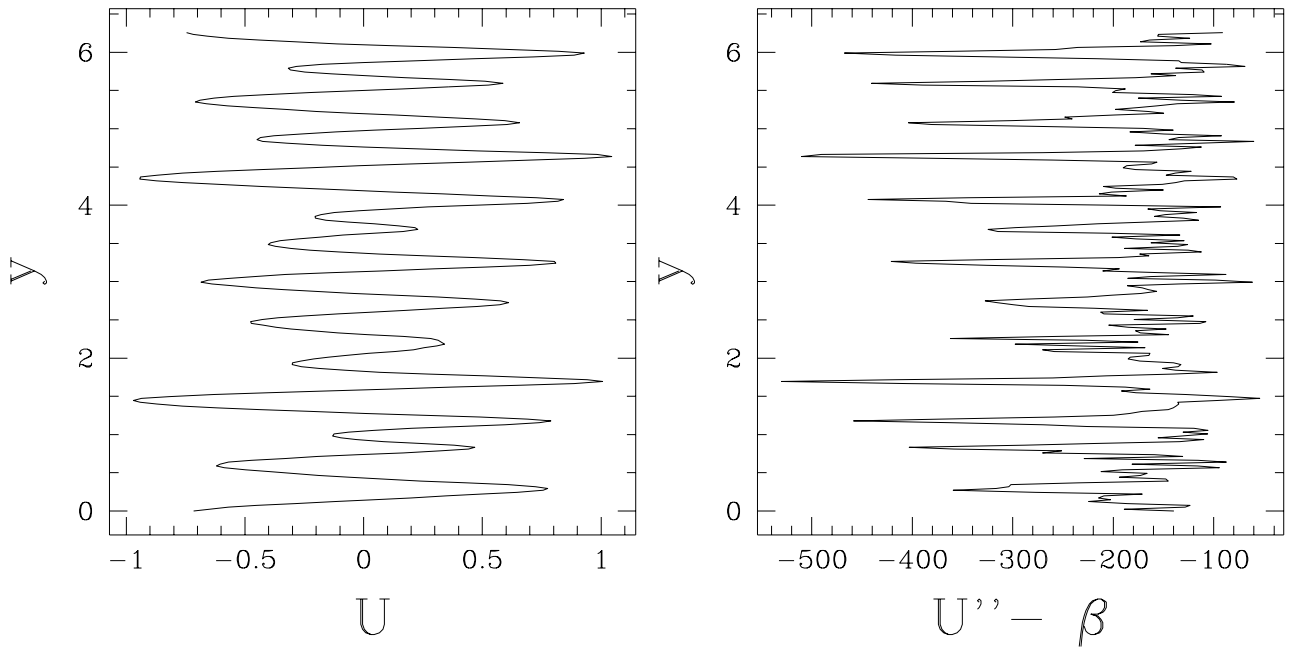

FIG. 1. Averaged zonal velocity U (a) and $U_{yy} - \beta$ (b) as functions of latitude y.

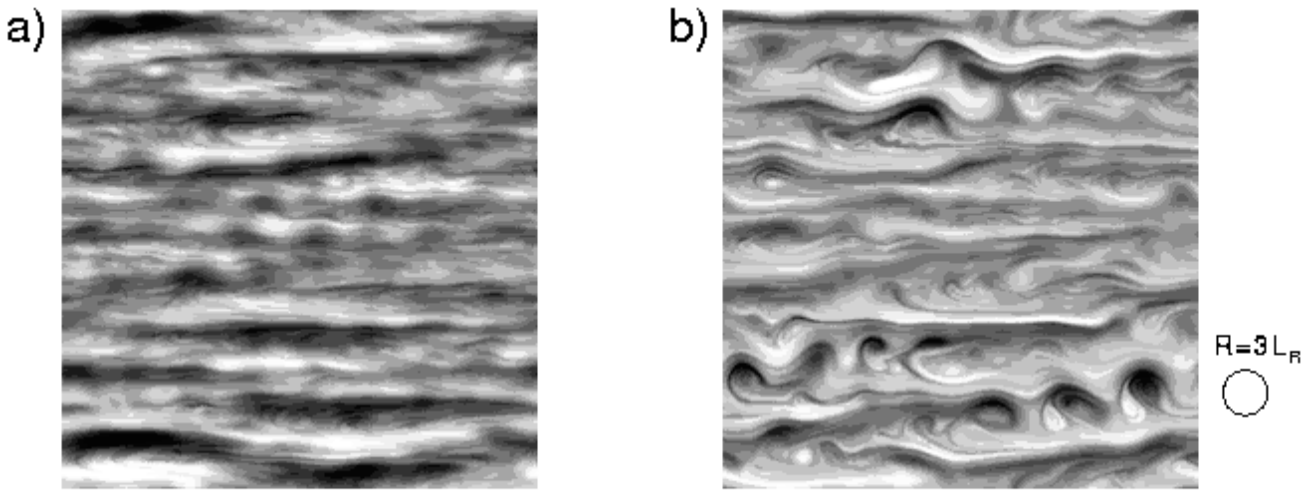

Figure 2: Finite deformation radius makes zonal flows unstable with respect to generation of anticyclones. The vorticity field before (a) and after (b) introducing a finite deformation radius L_R (whose scale is shown in the right picture). Darker colors correspond to anticyclones.

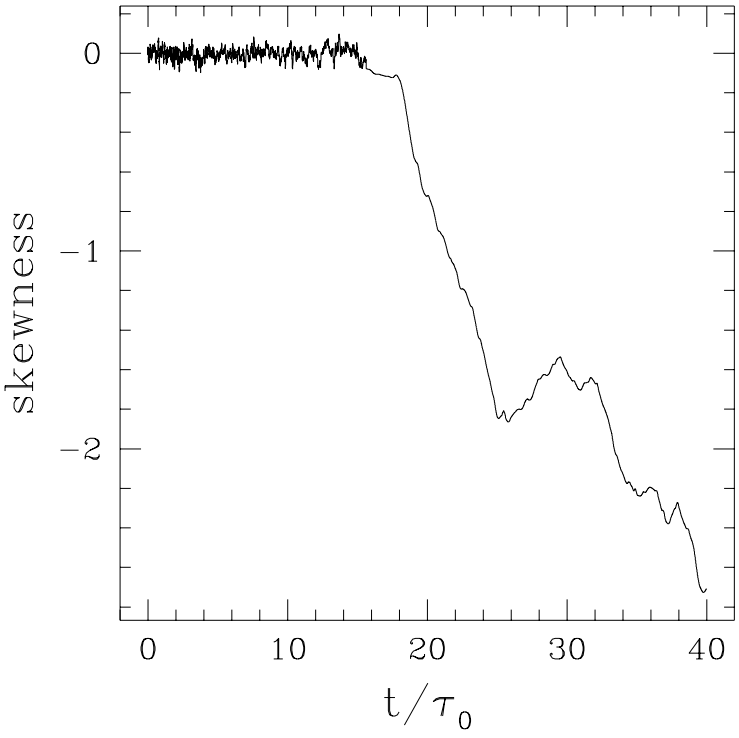

FIG.3. Vorticity skewness $S_\omega(t)$, $\lambda = 0$ before $t = 15\tau_0$ and $\lambda = 10$ afterwards.

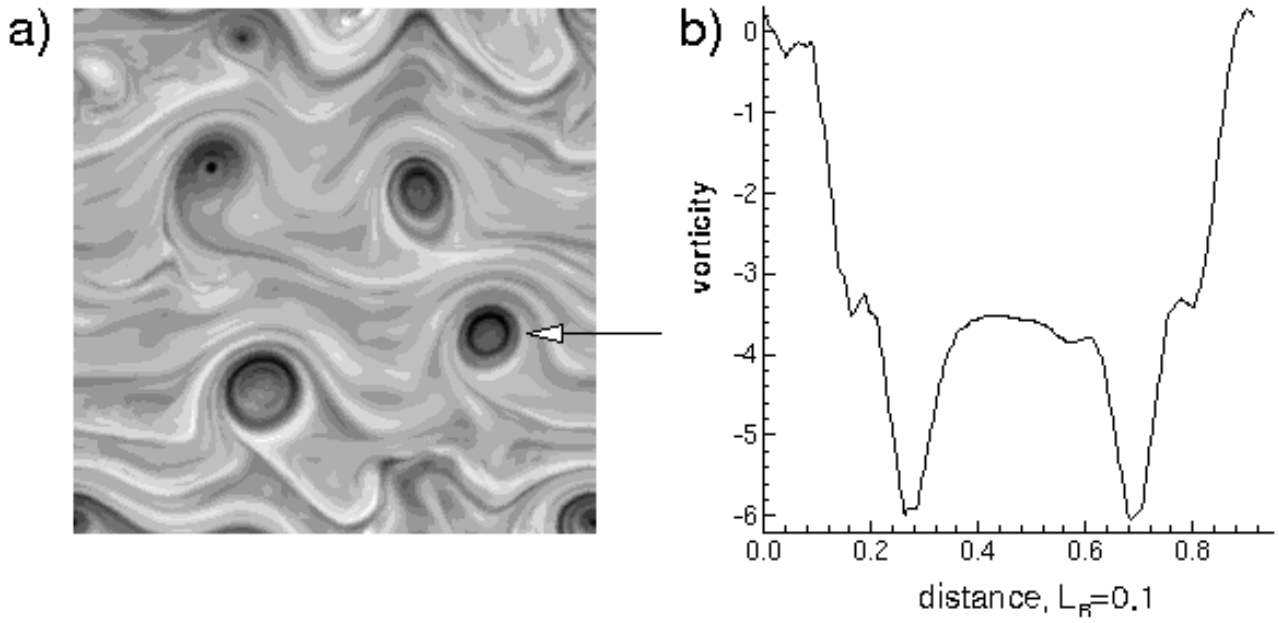

Figure 4: Instantaneous vorticity field at $t = 40\tau_0$ showing the ring anticyclonic vortices, $S_\omega = -2.8$ (a); cross section of a typical vortex (b).

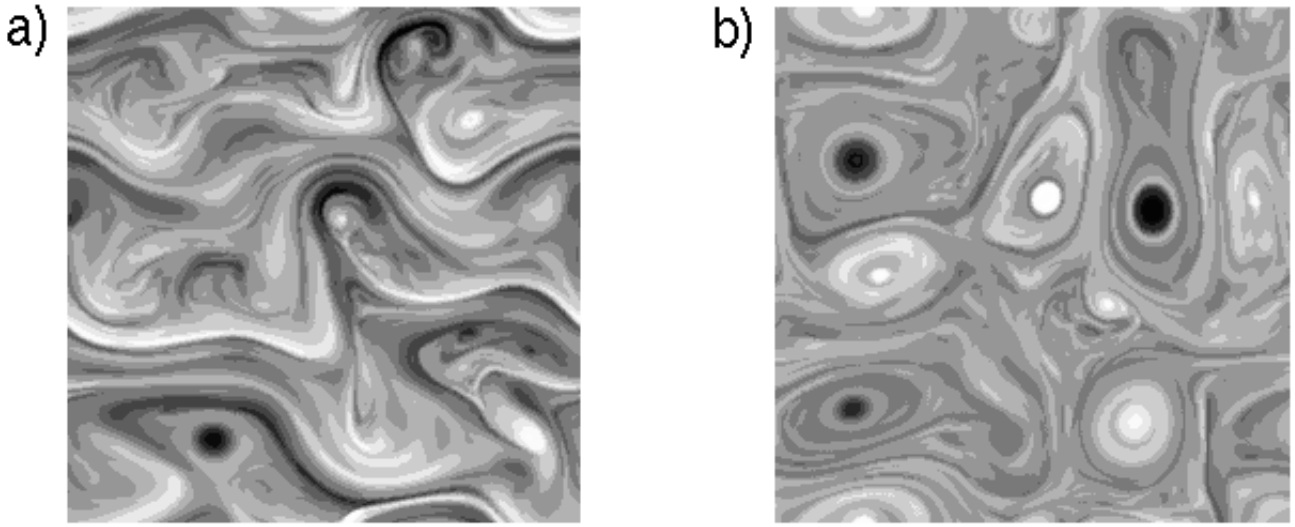

Figure 5: Vorticity fields at the same time as in Fig.4 when (a) the scalar nonlinearity is dropped, $S_\omega = 0$; (b) $\beta = 0$, but the term $J(h, h\nabla^2 h + \frac{1}{2}(\nabla h)^2)$ is added, $S_\omega = -0.3$.